JOC Article

Azacalix[7]arene Heptamethyl Ether: Preparation, Nanochannel Crystal Structure, and Selective Adsorption of Carbon Dioxide†

Hirohito Tsue,* Kazuhiro Matsui, Koichi Ishibashi, Hiroki Takahashi, Satoshi Tokita, Kohei Ono, and Rui Tamura

Graduate School of Human and Environmental Studies, Kyoto University, Sakyo-ku, Kyoto 606-8501, Japan

tsue@ger.mbox.media.kyoto-u.ac.jp

Received July 14, 2008

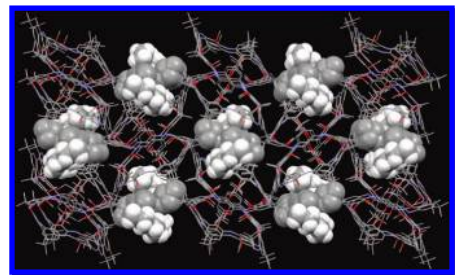

To investigate the solid-state complexation of nitrogen-bridged calixarene analogues, azacalix[7]arene heptamethyl ether **1** has been prepared by applying a "5 + 2"-fragment coupling approach using Buchwald−Hartwig aryl amination reaction aided by our previously devised temporal *N*-silylation protocol. X-ray crystallographic analysis revealed that azacalix[7]arene **1** adopted a highly distorted 1,2-alternate conformation in the solid state as a result of intramolecular NH/O hydrogen bonding interactions and steric repulsion between the methoxy groups. In the crystal, molecules of **1** are mutually interacted by intermolecular NH/O and CH/π interactions to establish one-dimensional (1D) hexane-filled nanochannel crystal architecture. Similarly to our recently reported azacalix[6]arene **2**, the desolvated crystalline powder material of **1** was capable of selectively and rapidly adsorbing CO_2 among the four main components of the atmosphere. The adsorption capacity of **1** for CO_2 nearly doubled as compared to that of **2** because of the formation of the 1D nanochannel with almost twice the volume of the latter.

Introduction

Over the past decades calixarenes have been playing an important role as a molecular receptor in host−guest chemistry because of their versatile ability to form inclusion complexes with a variety of organic and inorganic guests species.[1−4] An accumulated diverse knowledge on the host−guest chemistry of calixarenes in solution phase renders them further intriguing, coupled with their ease of synthesis and derivatization. Recently, there has been a marked development in the calixarene chemistry, in that solid−gas adsorption phenomenon has entered as a new research area in the host−guest study of calixarenes with the intention of achieving selective gas recognition, storage, and separation. Indeed, Atwood and Barbour demonstrated that *p-tert*-butylcalix[*n*]arenes (n = 4 and 5) were capable of efficiently adsorbing gaseous molecules on the apparently nonporous crystals under ambient conditions,[5] where the calixarenes exhibited greater adsorption ability as compared to those of metal-organic frameworks (MOFs) and carbon nanotubes.[5i] Similar gas adsorption behavior was observed for other calix[4]arene derivatives in which *tert*-pentyl and *tert*-octyl groups were introduced onto the upper rim.[5e]

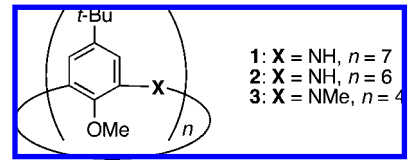

† This paper is dedicated to Professor Yoshiteru Sakata on the occasion of his 70th birthday.

(1) (a) Gutsche, C. D. *Calixarenes*; Stoddart, J. F., Ed.; The Royal Society of Chemistry: Cambridge, U.K., 1989. (b) Gutsche, C. D. *Calixarenes Revisited*; Stoddart, J. F., Ed.; The Royal Society of Chemistry: Cambridge, U.K., 1998.

(2) *Calixarenes: A Versatile Class of Macrocyclic Compounds*; Vicens, J., Böhmer, V., Eds.; Kluwer: Dordrecht, The Netherlands, 1991.

(3) *Calixarenes 2001*; Asfari, Z., Böhmer, V., Harrowfield, J., Vicens, J., Saadioui, M., Eds.; Kluwer: Dordrecht, The Netherlands, 2001.

(4) For a review on calix 7arene derivatives, see: Martino, M.; Neri, P. *Mini-Rev. Org. Chem.* **2004**, *1*, 219.

10.1021/jo801543z CCC: $40.75
Published on Web 08/23/2008

Very recently, we found that solid−gas adsorption was also feasible by a calixarene analogue involving nitrogen atoms as the bridging units.[6,7] After desolvation of the hexane clathrate of azacalix[6]arene **2**, the resultant crystalline powder material exhibited selective and rapid uptake of CO_2 among the four main gaseous components of the atmosphere. The adsorption capacity of **2** for CO_2 was comparable to or somewhat poorer than those of MOFs[8] and zeolites,[9] which similarly exhibited the selective adsorption of CO_2. In contrast, smaller azacalix[4]-arene **3**[10,11] gave rise to no uptake of CO_2 in the solid state. These foregoing experimental findings naturally compelled us to prepare a larger homologue. In the present study, to gain a deeper insight into the solid−gas adsorption behavior of this molecular system, we have synthesized azacalix[7]arene heptamethyl ether **1** with a larger ring size than in **2** and **3**. As in the case of **2**, selective and rapid adsorption of CO_2 was observed on the desolvated crystalline powder material of **1**, which was obtained from the single crystals of the hexane clathrate with a 1:2 host−guest ratio. To our knowledge, the present X-ray crystallographic analysis of **1** has provided the second instance[12] of solid-state structure in nitrogen-bridged calix[7]arene analogues reported to date.[12,13] More interestingly, it was also found that adsorption capacity of **1** for CO_2 was almost twice as much as that of **2**. In this paper, we report the synthesis, crystal structure, and solid−gas adsorption behavior of azacalix[7]arene **1**.

Results and Discussion

Synthesis. Preparation of azacalix[7]arene **1** was accomplished by using a convergent "5 + 2"-fragment coupling approach shown in Scheme 1. The "5"-fragment **10** was prepared according to our described procedure,[14] whereas the "2"-fragment **9** was newly synthesized via the following six reaction steps. Starting from hydrazine reduction of nitroanisole **4**[15] in 94% yield, the resultant aniline **5** was treated with Boc_2O to give monoprotected aniline **6** in 99% yield. Buchwald−Hartwig aryl amination reaction[16] of **6** and monoprotected *m*-phenylenediamine **7**[10] smoothly proceeded to furnish dimer **8** in 92% yield. The 2-fragment **9** was finally prepared by the additional protection of the terminal amino groups of **8** with Boc_2O in the presence of DMAP, followed by the *N*-benzylation of the bridging nitrogen atom and by the removal of all Boc groups with TFA. Buchwald−Hartwig aryl amination reaction using a temporal *N*-silylation protocol[17] was applied to the ring-closing reaction of 5-fragment **10** with 2-fragment **9**. From this macrocyclization reaction, regioselectively pentabenzylated azacalix[7]arene **11** was obtained in 33% yield through the in situ *N*,*N*′-bissilylation of 2-fragment **9** with dimethylphenylsilyl chloride (DMPSCl) in the presence of *t*-BuONa, followed by the one-pot Pd(0)-catalyzed aryl amination reaction with 5-fragment **10** and by the subsequent cleavage of N−Si bond in the workup process. As a final step, all the *N*-benzyl groups of **11** were deprotected by hydrogenolysis using 10% $Pd(OH)_2$/C as a catalyst to afford azacalix[7]arene **1** in 89% yield. HRMS, ^{1}H NMR, ^{13}C NMR, FT IR, elemental analysis, and X-ray crystallographic analysis fully characterized the structure of this new azacalix[7]arene **1**.

Crystal Structure. A single crystal of **1** was obtained by slow crystallization from hexane involving a few drops of CH_2Cl_2. Azacalix[7]arene **1** crystallizes with two molecules of hexane and adopts a highly distorted 1,2-alternate conformation in the solid state, as shown in Figure 1. As a result of intramolecular NH···OMe hydrogen bonding interactions, the aromatic rings **A**, **B**, **C**, **D**, and **E** are directed upward with respect to the mean plane defined by all of the bridging nitrogen atoms, whereas the remaining aromatic rings **F** and **G** are directed downward. The observed nonsymmetry of **1** is much different from our previously reported azacalix[6]arene **2** with S_2 symmetry in the solid state,[6] though both compounds involve essentially the same type of intramolecular NH/O hydrogen

(5) (a) Atwood, J. L.; Barbour, L. J.; Jerga, A. *Science* **2002**, *296*, 2367. (b) Atwood, J. L.; Barbour, L. J.; Jerga, A. *Angew. Chem., Int. Ed.* **2004**, *43*, 2948. (c) Atwood, J. L.; Barbour, L. J.; Thallapally, P. K.; Wirsig, T. B. *Chem. Commun.* **2005**, 51. (d) Thallapally, P. K.; Wirsig, T. B.; Barbour, L. J.; Atwood, J. L. *Chem. Commun.* **2005**, 4420. (e) Thallapally, P. K.; Lloyd, G. O.; Wirsig, T. B.; Bredenkamp, M. W.; Atwood, J. L.; Barbour, L. J. *Chem. Commun.* **2005**, 5272. (f) Dobrzanska, L.; Lloyd, G. O.; Raubenheimer, H. G.; Barbour, L. J. *J. Am. Chem. Soc.* **2006**, *128*, 698. (g) Thallapally, P. K.; Dorbrzanska, L.; Gingrich, T. R.; Wirsig, T. B.; Barbour, L. J.; Atwood, J. L. *Angew. Chem., Int. Ed.* **2006**, *45*, 6506. (h) Thallapally, P. K.; Dalgarno, S. J.; Atwood, J. L. *J. Am. Chem. Soc.* **2006**, *128*, 15060. (i) Thallapally, P. K.; Kirby, K. A.; Atwood, J. L. *New J. Chem.* **2007**, *31*, 628. (j) Dalgarno, S. J.; Thallapally, P. K.; Barbour, L. J.; Atwood, J. L. *Chem. Soc. Rev.* **2007**, *36*, 236. (k) Thallapally, P. K.; McGrail, B. P.; Atwood, J. L. *Chem. Commun.* **2007**, 1521. (l) Thallapally, P. K.; McGrail, B. P.; Atwood, J. L.; Gaeta, C.; Tedesco, C.; Neri, P. *Chem. Mater.* **2007**, *19*, 3355. (m) Dalgarno, S. J.; Tian, J.; Warren, J. E.; Clark, T. E.; Makha, M.; Raston, C. L.; Atwood, J. L. *Chem. Commun.* **2007**, 4848. (n) Thallapally, P. K.; McGrail, B. P.; Dalfarno, S. J.; Schaef, H. T.; Tian, J.; Atwood, J. L. *Nat. Mater.* **2008**, *7*, 146.

(6) Tsue, H.; Ishibashi, K.; Tokita, S.; Takahashi, H.; Matsui, K.; Tamura, R. *Chem. Eur. J.* **2008**, *14*, 6125.

(7) For a review on nitrogen-bridged calixarene analogues, see: Tsue, H.; Ishibashi, K.; Tamura, R. In *Heterocyclic Supramolecules I*; Matsumoto, K., Ed.; Springer-Verlag: Berlin, Heidelberg, 2008; *Topics in Heterocyclic Chemistry*, Vol. *17*, pp 73−96.

(8) (a) Pan, L.; Adams, K. M.; Herrandez, H. E.; Wang, X.; Zheng, C.; Hattori, Y.; Kaneko, K. *J. Am. Chem. Soc.* **2003**, *125*, 3062. (b) Dybtsev, D. N.; Chun, H.; Yoon, S. H.; Kim, D.; Kim, K. *J. Am. Chem. Soc.* **2004**, *126*, 32. (c) Humphrey, S. M.; Chang, J.-S.; Jhung, S. H.; Yoon, J. W.; Wood, P. T. *Angew. Chem., Int. Ed.* **2006**, *46*, 272. (d) Llewellyn, P. L.; Bourrelly, S.; Serre, C.; Filinchuk, Y.; Férey, G. *Angew. Chem., Int. Ed.* **2006**, *46*, 7752. (e) Ma, S.; Sun, D.; Wang, X.-S.; Zhou, H.-C. *Angew. Chem., Int. Ed.* **2007**, *46*, 2458. (f) Sung, J. W.; Jhung, S. H.; Hwang, Y. K.; Humphrey, S. M.; Wood, P. T.; Chang, J.-S. *Adv. Mater.* **2007**, *19*, 1830. (g) Chen, B.; Ma, S.; Zapata, F.; Fronczek, F. R.; Lobkovsky, E. B.; Zhou, H.-C. *Inorg. Chem.* **2007**, *46*, 1233. (h) Zou, Y.; Hong, S.; Park, M.; Chun, H.; Lah, S. *Chem. Commun.* **2007**, 5182. (i) Bong, B.; Câté, A. P.; Furukawa, H.; O'Keeffe, M.; Yaghi, O. M. *Nature* **2008**, *453*, 207.

(9) (a) Choudhary, V. R.; Mayadevi, S.; Singh, A. P. *J. Chem. Soc., Faraday Trans.* **1995**, *91*, 2935. (b) Dunne, J. A.; Rao, M.; Sircar, S.; Gorte, R. J.; Myers, A. L. *Langmuir* **1996**, *12*, 5896. (c) Katoh, M.; Yoshikawa, T.; Tomonari, T.; Katayama, K.; Tomida, T. *J. Colloid Interface Sci.* **2000**, *226*, 145. (d) Siriwardane, R. V.; Shen, M.-S.; Fischer, E. P.; Poston, J. A. *Energy Fuels* **2000**, *15*, 279. (e) Paksesresht, S.; Kazemeini, M.; Akbarnejad, M. M. *Sep. Purif. Technol.* **2002**, *28*, 53. (f) Akten, E. D.; Siriwardane, R.; Sholl, D. S. *Energy Fuels* **2003**, *17*, 977. (g) Bonenfant, D.; Kharoune, M.; Niquette, P.; Mimeault, M.; Hausler, R. *Sci. Technol. Adv. Mater.* **2008**, *9*, 13007.

(10) Tsue, H.; Ishibashi, K.; Takahashi, H.; Tamura, R. *Org. Lett.* **2005**, *7*, 2165.

(11) Azacalix[4]arene **3** with NMe bridges was employed for comparison because the synthesis of an azacalix[4]arene with NH bridges is under progress.

(12) For the first X-ray crystallographic analysis of nitrogen-bridged calix[7]arene analogue, see: Zhang, E.-X.; Wang, D.-X.; Zheng, Q.-Y.; Wang, M.-X. *Org. Lett.* **2008**, *10*, 2565.

(13) (a) Ito, A.; Ono, Y.; Tanaka, K. *New J. Chem.* **1998**, 779. (b) Ito, A.; Ono, Y.; Tanaka, K. *J. Org. Chem.* **1999**, *64*, 8236. (c) Suzuki, Y.; Yanagi, T.; Kanbara, T.; Yamamoto, T. *Synlett* **2005**, 263.

(14) Ishibashi, K.; Tsue, H.; Sakai, N.; Tokita, S.; Matsui, K.; Yamauchi, J.; Tamura, R. *Chem. Commun.* **2008**, 2812.

(15) Hao, M.-H.; Xiong, Z.; Aungst, R. A.; Davis, A. L.; Cogan, D.; Goldberg, D. R. *U.S. Pat. Appl. Publ. 2005245536*, 2005; *Chem. Abstr.* **2005**, *143*, 1177572.

(16) For reviews on palladium(0)-catalyzed aryl amination reaction, see:(a) Wolfe, J. P.; Wagaw, S.; Marcoux, J. F.; Buchwald, S. L. *Acc. Chem. Res.* **1998**, *31*, 805. (b) Hartwig, J. F. *Acc. Chem. Res.* **1998**, *31*, 852. (c) Hartwig, J. F. *Angew. Chem., Int. Ed.* **1998**, *37*, 2046. (d) Muci, A. R.; Buchwald, S. L. *Top. Curr. Chem.* **2002**, *219*, 133.

(17) Ishibashi, K.; Tsue, H.; Tokita, S.; Matsui, K.; Takahashi, H.; Tamura, R. *Org. Lett.* **2006**, *8*, 5991.

(18) Kranenburg, M.; van der Burgt, Y. E. M.; Kamer, P. C. J.; van Leeuwen, P. W. N. M.; Goubitz, K.; Fraanje, J. *Organometallics* **1995**, *14*, 3081.

SCHEME 1. Preparation of Azacalix[7]arene 1[a]

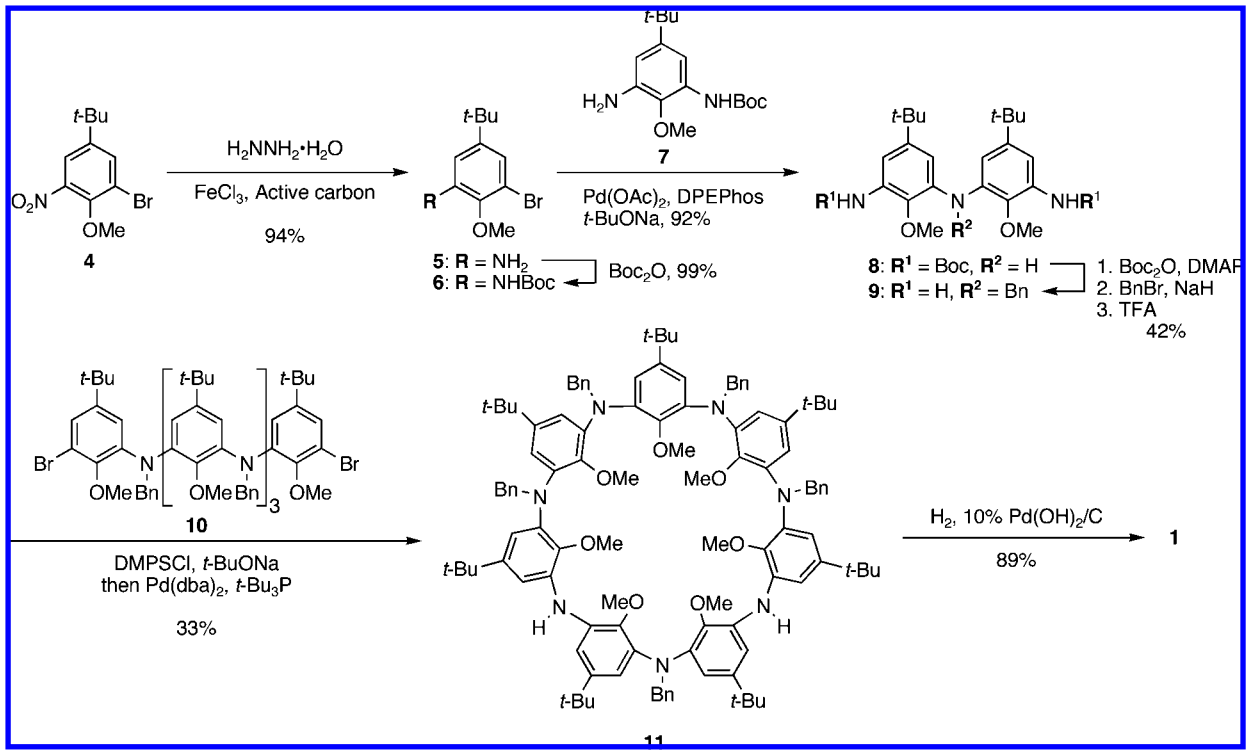

[a] DPEphos = bis[2-(diphenylphosphino)phenyl] ether.[18]

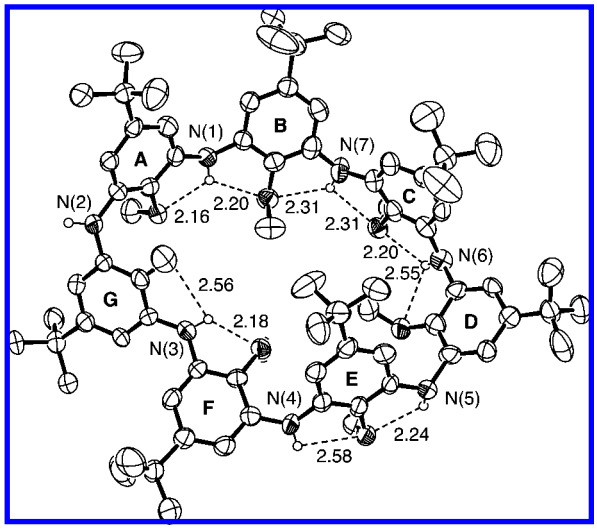

FIGURE 1. ORTEP drawing[19] of azacalix[7]arene **1**. The displacement ellipsoids are drawn at the 50% probability level. Solvent molecules and all hydrogen atoms but for the bridging NH groups are omitted for clarity. Numbers indicate O···H distances (Å) of intramolecular NH···OMe hydrogen bonds.

bonds. A conclusive difference between **1** and **2** is the spatial arrangements of the methoxy groups. In azacalix[6]arene **2**, each methoxy group is always oriented to the opposite direction from the neighboring ones to avoid steric hindrance between them. This is also the case for azacalix[4]arene **3** with apparent D_{2d} symmetry in the crystal.[10] In contrast, such regularly alternating arrangement of the methoxy groups is fundamentally unfeasible in azacalix[7]arene **1** because of the presence of an odd number of methoxy groups. In fact, the aromatic ring **E** of **1** is fluctuated to avoid the close proximity of the methoxy groups attached to the aromatic rings **D** and **E**, thereby lowering the molecular symmetry of **1**. As a result, the molecular structure of **1** in the solid state is controlled not only by intramolecular NH/O hydrogen bonding interactions but also by the inevitable collapse of the favorable alternate arrangement of the methoxy groups. Of seven NH hydrogens of **1**, six are involved in the formation of *intra*molecular NH/O hydrogen bonds, whereas the remaining one at N(2) atom takes part in the formation of *inter*molecular hydrogen bonds mentioned below.

Also interesting is the crystal packing characterized by hexane-filled one-dimensional (1D) nanochannel crystal architecture shown in Figure 2. In the crystal, each azacalix[7]arene **1** is mutually interacted with adjacent molecules by intermolecular NH···OMe hydrogen bonds formed between the bridging nitrogen atoms N(2) and the methoxy groups of the aromatic ring **E** belonging to the neighboring molecule (type α, N···O, 3.05 Å; NH···O, 2.29 Å and 148.1°), as depicted in Figure 3a. By virtue of the intermolecular NH/O hydrogen bonds, a 1D chain structure is formed along the crystallographic *b* axis in an antiparallel direction. Besides, the 1D chains interact with each other by intermolecular CH/π interactions formed between the methoxy groups located on the rings **C** and the centroid of the rings **F** belonging to the nearest molecules (type β, C···centroid 3.47 Å, CH···centroid 2.73 Å and 133.1°), as shown in Figure 3b. As a consequence of the intermolecular NH/O and CH/π interactions, a two-dimensional (2D) sheet structure of **1** is eventually formed on the *bc* plane, as schematically illustrated in Figure 3c. In the 2D sheet structure, each molecular assembly comprising six molecules of **1** creates an interstitial pore (465 Å^3), in which four molecules of hexane are embedded. As a result, the hexane-filled 2D sheet structure is stacked along the *a* axis to form the 1D nanochannel crystal architecture of the hexane clathrate of **1** with a 1:2 host−guest

(19) Farrugia, L. J. *J. Appl. Crystallogr.* **1997**, *30*, 565.

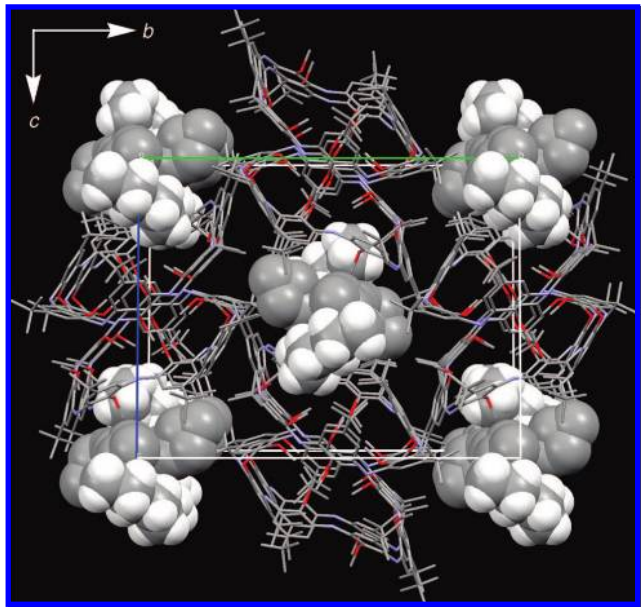

FIGURE 2. Crystal structure of the hexane clathrate of azacalix[7]arene **1** viewed along the crystallographic *a* axis. Molecules of azacalix[7]arene **1** and hexane are represented by stick and space-filling models, respectively. Hydrogen atoms except for those of nondisordered hexane are omitted for clarity. Hydrogen atoms of disordered hexane are not included in the crystallographic calculation.

ratio, as shown in Figure 2. Azacalix[6]arene **2** also forms a similar hexane-filled 1D nanochannel crystal structure,[6] but the interstitial void space of **1** is almost twice as large as that of **2** (208 Å^3) because the highly distorted conformation of **1** (Figure 1) probably leads to the less efficient packing in the crystal than **2**.

Solid−Gas Adsorption Behavior. For the sake of desolvation, single crystals of the hexane clathrate of **1** were heated at 30 °C for 24 h under reduced pressure. As shown in Figure 4b, no ^{1}H NMR signal of hexane was observed after the desolvation procedure, indicating the complete escape of the molecules of hexane from the single crystals of **1**. After desolvation, however, the hexane clathrate of **1** lost the single crystallinity and turned to crystalline powder **1P**. The letter "**P**" is used below to represent the solvent-free powder material obtained from the single crystals of the hexane clathrate of **1**.

To gain an insight into the crystallographic aspect of **1P**, the synchrotron powder X-ray diffraction (XRD) data was collected at the BL02B2 beamline of the Super Photon Ring (SPring-8, Hyogo, Japan).[20] The crystal structure of **1P** could not be solved from the XRD pattern at this moment, but the lattice parameters of **1P** were found to be almost identical to those of the hexane clathrate of **1**, as summarized in Table 1. This essential agreement is clearly reflected in the XRD pattern of **1P** (Figures 5a and S13 in Supporting Information), which displays a dissimilarity to that simulated from the X-ray crystallographic data of the hexane clathrate of **1** (Figure 5b) but a similarity to that simulated from the imaginary crystal structure simply created by deleting the atomic coordinates of hexane from the crystallographic data of the hexane clathrate (Figure 5c). Furthermore, FT IR measurement of **1P** revealed no appreciable changes in the NH-stretching, NH-bending, and CN-stretching bands even after the loss of single crystallinity (Figure 6),

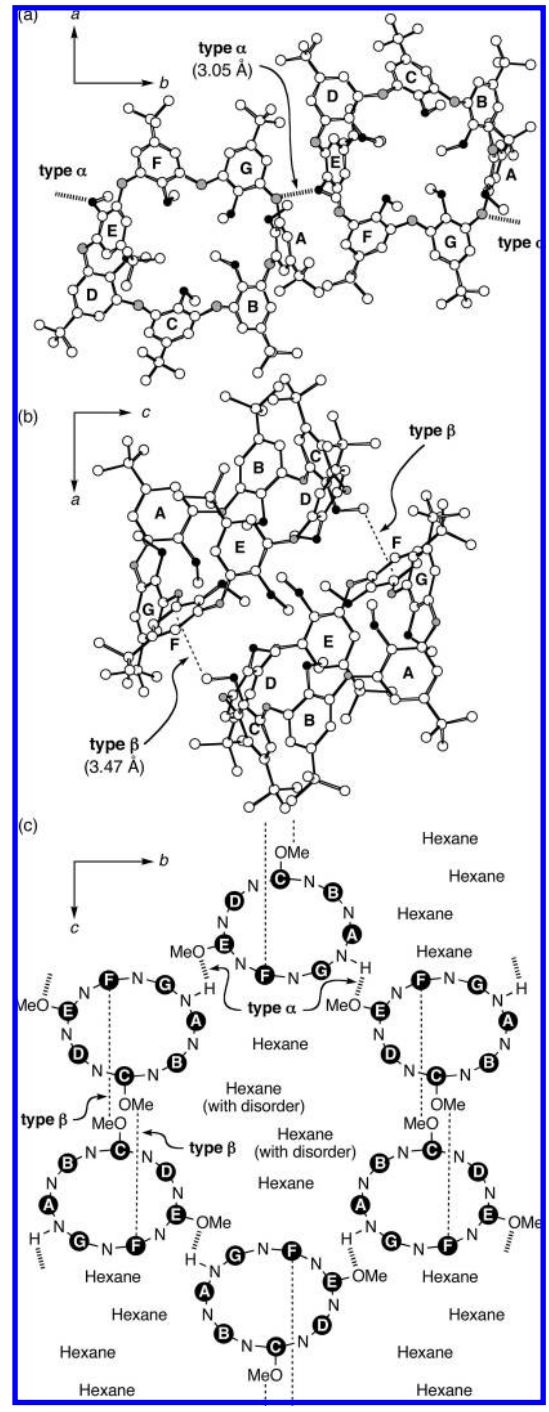

FIGURE 3. Crystal structure of the hexane clathrate of azacalix[7]arene **1** viewed along (a) the *c* axis and (b) the *b* axis. The carbon, nitrogen, and oxygen atoms are represented by open, shaded, and closed circles, respectively. The two-dimensional structure on the *bc* plane is schematically illustrated in panel (c), where the aromatic rings from **A** to **G** are represented by closed circles with lettering. For clarity, only the functional groups are depicted that are involved in the formation of intermolecular NH/O and CH/π interactions. Panel c schematically illustrates the arrangement of the molecules in the unit cell shown in Figure 2.

suggesting that the 1D nanochannel structure shown in Figure 2 remained almost unchanged in **1P**. From these experimental facts, it is conceivable that, upon heating the single crystals of the hexane clathrate of **1**, molecules of hexane escape through the 1D nanochannel almost keeping the intra- and intermolecular

(20) Nishibori, E.; Takata, M.; Kato, K.; Sakata, M.; Kubota, Y.; Aoyagi, S.; Kuroiwa, Y.; Yamakata, M.; Ikeda, N. *J. Phys. Chem. Solids* **2001**, *62*, 2095.

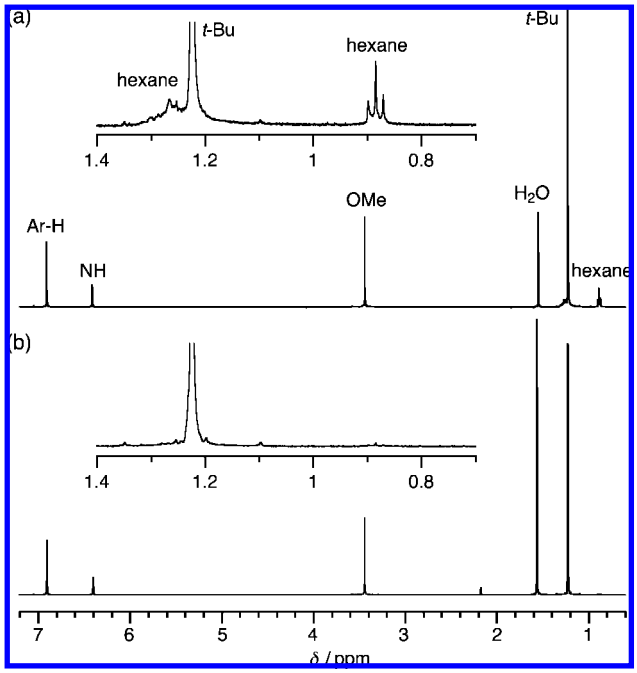

FIGURE 4. ^{1}H NMR spectra taken in $CDCl_3$ (a) before and (b) after heating the single crystals of the hexane clathrate of azacalix[7]arene **1** at 30 °C for 24 h under reduced pressure.

TABLE 1. Crystallographic Data of Desolvated Crystalline Powder 1P and the Single Crystal of the Hexane Clathrate of 1

	1P	**1**·2hexane
crystal system	monoclinic	monoclinic
space group	$P2_1/c$	$P2_1/c$
a (Å)	17.879	18.458(1)
b (Å)	24.487	24.536(2)
c (Å)	19.198	19.523(1)
β (deg)	103.030	101.494(2)
V (Å^3)	8189	8664(1)

NH/O hydrogen bonding interactions as well as the intermolecular CH/π-interactions.

To examine the ability of **1P** as a nanoporous material, adsorption experiments for gaseous molecules were carried out. According to the described procedure,[5c] adsorption isotherms for the four main atmospheric components such as N_2, O_2, Ar, and CO_2 were recorded at room temperature and 195 K on the desolvated powder **1P**. The initial pressure was set to ca. 100 kPa in all adsorption experiments. As shown in Figure 7a, almost no uptake was observed for all of the examined gases at room temperature. In contrast, CO_2 was rapidly and selectively adsorbed on **1P** at 195 K (Figure 7b), and the initial pressure of ca. 100 kPa was decreased within 20 min to reach equilibrium at 34 kPa, corresponding to the uptake of 3.0 mol of CO_2 per mol of **1** (i.e., 55 cm^3 g^{-1} at standard temperature and pressure). It is interesting to note that the observed adsorption capacity of **1P** for CO_2 is almost comparable to those of MOFs[8] and zeolites[9] capable of selectively adsorbing CO_2, though the adsorption of CO_2 on **1P** only takes place at 195 K. It is also noteworthy that the adsorption capacity of **1P** for CO_2 is nearly twice as much as that of our recently reported azacalix[6]arene **2** (1.8 mol of CO_2 per mole of **2**)[6] because the former creates the 1D nanochannel with almost twice the volume of the latter.

Because the observed gas adsorption behavior of **1P** at 195 K is essentially the same as that of **2** except for the adsorption capacity, the selective and rapid uptake of CO_2 by **1P** at 195 K

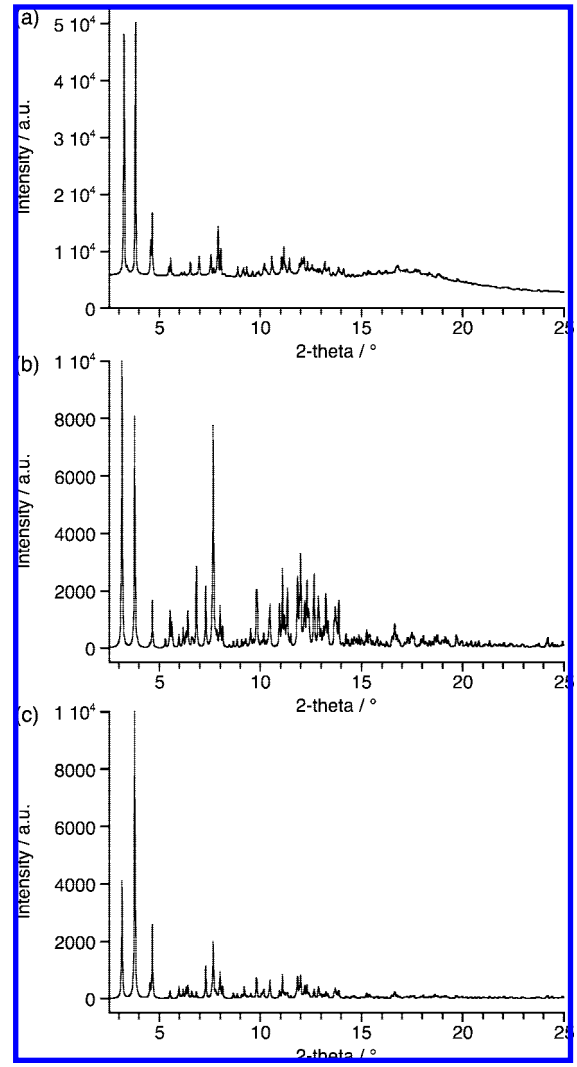

FIGURE 5. (a) Synchrotron powder X-ray diffraction (XRD) pattern of desolvated crystalline powder **1P**. (b) XRD pattern simulated from the X-ray crystallographic data of the hexane clathrates of **1**. (c) XRD pattern simulated from the imaginary crystal structure simply created by deleting the atomic coordinates of hexane from the crystallographic data of the hexane clathrate of **1**.

can be interpreted by considering the following three factors, as in the case of **2**.[6] The first is the molecular sieve effect based on the difference in the kinetic diameters of the examined gases such as N_2 (3.64 Å), O_2 (3.46 Å), Ar (3.40 Å), and CO_2 (3.3 Å),[21] the last of which is the smallest to ensure the easy diffusion into the 1D nanochannel of **1P**. The second is hydrogen bonding interactions between the NH hydrogen atoms and CO_2 molecules diffused into the 1D nanochannel of **1P**. This is parallel to our previous experimental facts that both azacalix[4]arene **3** and *p-tert*-butylcalix[6]arene hexamethyl ether give rise to almost no uptake of CO_2 even at 195 K because of the lack of hydrogen bonding sites, together with their densely packed crystal structures.[6,10] The third is the quadrupole/induced-dipole interactions between CO_2 and the surrounding aromatic "walls" built along the 1D nanochannel of **1P**, judging from the greater quadrupole moment (absolute value)[22] of CO_2 (13.4×10^{40} C

(21) Breck, D. W. *Zeolite Molecular Sieves*; John Wiley & Sons: New York, 1974; pp 633−645.
(22) Steele, W. *Chem. Rev.* **1993**, *93*, 2355.

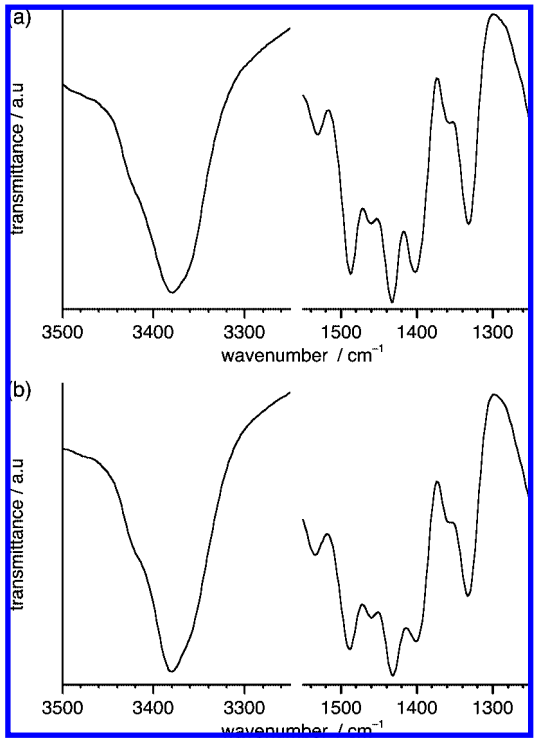

FIGURE 6. FT IR spectra of (a) desolvated crystalline powder **1P** and (b) single crystals of the hexane clathrate of **1**.

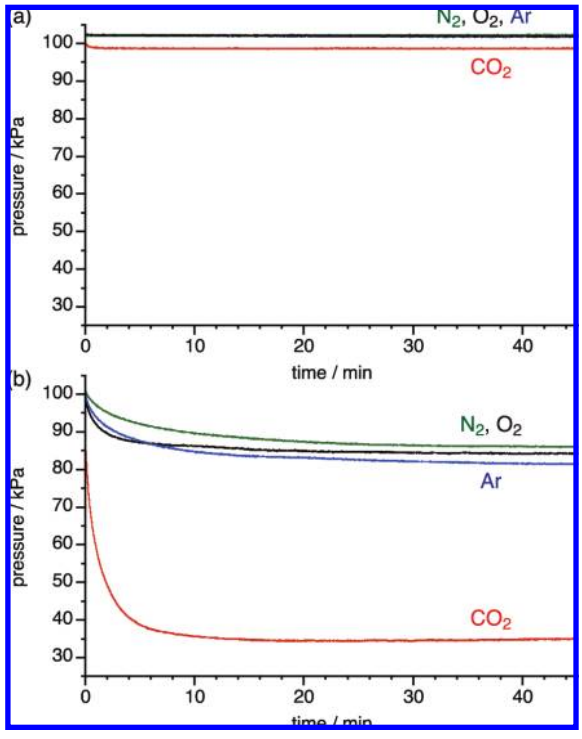

FIGURE 7. Gas adsorption isotherms recorded at (a) room temperature and (b) 195 K for N_2, O_2, Ar, and CO_2 using desolvated crystalline powder **1P** as adsorbent. Isotherms for N_2, O_2, Ar, and CO_2 are shown by green, black, blue, and red lines, respectively.

m^2) than the other examined gases such as N_2 (4.7×10^{40}), O_2 (1.3×10^{40}), and Ar (0). As a result, it is conceivable that a synergetic effect of these three factors is responsible for the observed selective and rapid uptake of CO_2 by **1P**.

Conclusions

We have demonstrated that azacalix[7]arene **1** can be prepared by using a Pd(0)-catalyzed aryl amination reaction, together with our previously devised temporal *N*-silylation protocol. X-ray crystallographic analysis clearly revealed that conformation of **1** in the solid state was controlled by intramolecular NH/O hydrogen bonding interactions and the inevitable collapse of the favorable alternating arrangement of the methoxy groups. In the crystal, molecules of **1** are mutually interacted by intermolecular NH/O hydrogen bonding interactions as well as the intermolecular CH/π-interactions to establish the infinite 1D nanochannel crystal architecture of the hexane clathrate of **1** with a 1:2 host−guest ratio. As in the case of azacalix[6]arene **2**, the desolvated powder **1P** was capable of selectively and rapidly adsorbing CO_2 among the four main components of the atmosphere. Because both azacalix[7]arene **1** and azacalix[6]arene **2** can selectively adsorb CO_2 in the solid state, we anticipate that their homologues with larger and/or smaller ring sizes may do so similarly to **1** and **2**. Investigations along this line are under progress to gain a more profound insight into the dynamic solid-state complexation of this molecular system.

Experimental Section

Palladium bis(benzylideneacetone) [$Pd(dba)_2$],[23] bis[2-(diphenylphosphino)phenyl] ether (DPEphos),[18] and compounds **4**,[14] **7**,[10] and **10**[14] were prepared according to the described procedures.

3-Bromo-5-*tert*-butyl-2-methoxyaniline (5). A solution of **4** (11.5 g, 39.9 mmol), $FeCl_3 \cdot 6H_2O$ (569 mg, 2.11 mmol), and active carbon (1.20 g) in MeOH (120 mL) was refluxed for 30 min. After $H_2NNH_2 \cdot H_2O$ (10.3 g, 206 mmol) was added dropwise to the flask, the mixture was heated under reflux for 1 h. The reaction mixture was cooled to room temperature, passed through Celite, evaporated, and extracted with CH_2Cl_2. The organic layer was washed with saturated $NaHCO_3$, dried over anhydrous K_2CO_3, filtered, and evaporated. Flash column chromatography on silica gel (hexane/CH_2Cl_2 = 1:1, v/v) afforded **5** (9.71 g, 94%) as colorless solid, mp 48−49 °C; ^{1}H NMR ($CDCl_3$, 500 MHz) δ 6.91 (d, J = 2.1 Hz, 1H, Ar−H), 6.69 (d, J = 2.1 Hz, 1H, Ar−H), 3.87 (br s, 2H, NH_2), 3.82 (s, 3H, OMe), 1.26 (s, 9H, *t*-Bu); ^{13}C NMR (125 MHz, $CDCl_3$) δ 149.1, 141.9, 140.5, 119.6, 116.5, 112.5, 59.5, 34.4, 31.2; IR (KBr) 3480, 3368 (ν_{N-H}) cm^{-1}. Anal. Calcd for $C_{11}H_{16}BrNO$: C, 51.18; H, 6.25; N, 5.43. Found: C, 51.14; H, 6.05; N, 5.47.

***tert*-Butyl (3-Bromo-5-*tert*-butyl-2-methoxyphenyl) Carbamate (6).** To a solution of **5** (2.58 g, 10.0 mmol) in *t*-BuOH (10 mL) was added Boc_2O (2.40 g, 11.0 mmol) in *t*-BuOH (5 mL). After stirring for 3 h at room temperature, the reaction mixture was evaporated and extracted with EtOAc. The organic layer was washed with saturated $NaHCO_3$, dried over anhydrous Na_2SO_4, filtered, and evaporated. Flash column chromatography on silica gel (hexane/CH_2Cl_2 = 1:1, v/v) yielded **6** (3.55 g, 99%) as colorless solid, mp 132−134 °C; ^{1}H NMR (500 MHz, $CDCl_3$) δ 8.10 (br s, 1H, NHBoc), 7.17 (d, 2H, J = 1.8 Hz, Ar−H), 7.00 (br s, 2H, Ar−H), 3.83 (s, 3H, OMe), 1.54 (s, 9H, *t*-Bu), 1.30 (s, 9H, *t*-Bu); ^{13}C NMR (125 MHz, $CDCl_3$) δ 152.8, 148.2, 138.3, 133.5, 131.4, 107.7, 106.5, 80.3, 59.3, 34.6, 31.4, 28.4; IR (KBr) 3428 (ν_{N-H}), 1730 ($\nu_{C=O}$) cm^{-1}. Anal. Calcd for $C_{16}H_{24}BrNO_3$: C, 53.64; H, 6.75; N, 3.91. Found: C, 53.38; H, 6.72; N, 3.86.

Di-*tert*-butyl [3,3′-Iminobis(5-*tert*-butyl-2-methoxyphenyl)] Dicarbamate (8). A solution of **6** (2.16 g, 6.03 mmol), **7** (1.77 g, 6.00 mmol), $Pd(OAc)_2$ (67.5 mg, 301 μmol), DPEphos (242.5 mg, 450 μmol), and *t*-BuONa (693 mg, 7.21 mmol) in anhydrous toluene (12 mL) was stirred at 80 °C for 23 h under Ar. After cooling to

(23) Ukai, T.; Kawazura, H.; Ishii, Y.; Bonnet, J. J.; Ibers, J. A. *J. Organomet. Chem.* **1974**, *65*, 253.

room temperature, the reaction mixture was passed through Celite, evaporated, and dried in vacuo. Flash column chromatography on silica gel (hexane/CH_2Cl_2 = 1:2, v/v) gave **8** (3.14 g, 92%) as colorless solid, mp 124−125 °C; ^{1}H NMR (500 MHz, $CDCl_3$) δ 7.70 (br s, 2H, NHBoc), 7.05 (d, J = 2.3 Hz, 2H, Ar−H), 6.96 (br s, 2H, Ar−H), 6.09 (br s, 1H, NH), 3.75 (s, 6H, OMe), 1.55 (s, 18H, *t*-Bu), 1.30 (s, 18H, *t*-Bu); ^{13}C NMR (125 MHz, $CDCl_3$) δ 152.8, 147.8, 135.8, 134.8, 131.7, 108.8, 108.6, 80.4, 60.1, 34.9, 31.4, 28.4; IR (KBr) 3431, 3387, 3358 (ν_{N-H}), 1728 ($\nu_{C=O}$) cm^{-1}. Anal. Calcd for $C_{32}H_{49}N_3O_6\cdot 0.2H_2O$: C, 66.80; H, 8.65; N, 7.30. Found: C, 66.67; H, 8.43; N, 7.30.

Bis(3-amino-5-*tert*-butyl-2-methoxyphenyl)-*N*-benzylamine (9). To a solution of **8** (2.74 g, 4.80 mmol) and DMAP (120 mg 985 μmol) in anhydrous THF (50 mL) was added Boc_2O (3.14 g, 14.4 mmol) in anhydrous THF (10 mL). The mixture was heated under reflux for 15 h. After cooling to room temperature, the reaction mixture was extracted with Et_2O. The organic layer was washed with saturated $NaHCO_3$, dried over anhydrous K_2CO_3, filtered, and evaporated. Flash column chromatography on silica gel (hexane/EtOAc = 4:1, v/v) afforded colorless solid. The solid was dissolved in anhydrous DMF (15 mL), and 60% NaH (301 mg, 7.53 mmol) was added at 0 °C under Ar. After stirring for 15 min, BnBr (884 mg, 5.63 mmol) was added. Stirring was continued at room temperature for 5 h, and then CH_2Cl_2 was added to the reaction mixture. The organic layer was washed with brine, dried over anhydrous Na_2SO_4, filtered, and evaporated. To the resultant residue CH_2Cl_2 (10 mL) and TFA (8 mL) were added, and the solution was stirred at room temperature for 1.5 h. After cooling to 0 °C, the reaction mixture was made basic to pH 11 with 5% aqueous NaOH and extracted with CH_2Cl_2. The organic layer was dried over anhydrous K_2CO_3, filtered, and evaporated. Flash column chromatography on silica gel (hexane/EtOAc = 4:1, v/v) afforded **9** (922 mg, 42%) as colorless solid, mp 158−159 °C; ^{1}H NMR (500 MHz, $CDCl_3$) δ 7.38 (d, J = 7.4 Hz, 2H, Ar−H), 7.24 (t, J = 7.4 Hz, 2H, Ar−H), 7.15 (d, J = 7.4 Hz, 1H, Ar−H), 6.51 (d, J = 2.3 Hz, 2H, Ar−H), 6.45 (d, J = 2.3 Hz, 2H, Ar−H), 4.86 (s, 2H, CH_2Ph), 3.66 (br s, 4H, NH_2), 3.54 (s, 6H, OMe), 1.17 (s, 18H, *t*-Bu); ^{13}C NMR (125 MHz, $CDCl_3$) δ 146.7, 142.1, 139.9, 139.7, 139.1, 128.04, 128.01, 126.5, 112.1, 108.0, 59.0, 57.6, 34.3, 31.3; IR (KBr) 3449, 3428, 3327 (ν_{N-H}) cm^{-1}. Anal. Calcd for $C_{29}H_{39}N_3O_2\cdot 0.3H_2O$: C, 74.56; H, 8.55; N, 8.99. Found: C, 74.45; H, 8.41; N, 8.89.

2,8,14,26,38-Pentabenzyl-5,11,17,23,29,35,41-hepta-*tert*-butyl-43,44,45,46,47,48,49-heptamethoxy-2,8,14,20,26,32,38-heptaazacalix[7]arene (11). A solution of **9** (46.5 mg, 101 μmol), **10** (141 mg, 101 μmol), *t*-BuONa (48.1 mg, 500 μmol), and dimethylphenylsilyl chloride (DMPSCl) (38.1 mg, 223 μmol) in anhydrous toluene (20 mL) was stirred at 80 °C under Ar. After stirring for 30 min, $Pd(dba)_2$ (12.0 mg, 20.9 μmol) and 10 wt% *t*-Bu_3P in hexane (50 μL, 16.7 μmol) were added. A solution was refluxed for 17 h and then cooled to room temperature. The reaction mixture was passed through Celite and evaporated. Flash column chromatography on silica gel (hexane/CH_2Cl_2 = 1:1, v/v) gave **11** (56.9 mg, 33%) as colorless solid, mp 162−164 °C; ^{1}H NMR (500 MHz, $CDCl_3$, 55 °C) δ 7.44 (d, J = 7.3 Hz, 2H, Ar−H), 7.34 (d, J = 7.3 Hz, 4H, Ar−H), 7.28−7.04 (m, 19H, Ar−H), 6.83 (d, J = 2.1 Hz, 2H, Ar−H), 6.81 (d, J = 1.8 Hz, 2H, Ar−H), 6.73 (d, J = 2.1 Hz, 2H, Ar−H), 6.69 (d, J = 2.1 Hz, 2H, Ar−H), 6.61 (br s, 2H, Ar−H), 6.59 (br s, 2H, Ar−H), 6.58 (d, J = 2.1 Hz, 2H, Ar−H), 5.95 (s, 2H, NH), 4.90 (s, 2H, CH_2Ph), 4.87 (s, 4H, CH_2Ph), 4.78 (s, 4H, CH_2Ph), 3.41 (br s, 6H, OMe), 3.25 (br s, 6H, OMe), 3.15 (s, 6H, OMe), 3.13 (s, 3H, OMe), 1.16 (s, 18H, *t*-Bu), 1.11 (s, 18H, *t*-Bu), 1.01 (s, 18H, *t*-Bu), 0.98 (s, 9H, *t*-Bu); ^{13}C NMR (125 MHz, $CDCl_3$, 55 °C) δ 146.1, 145.9, 145.5, 145.1, 145.0, 143.5, 143.1, 142.4, 141.6, 140.2, 140.0, 139.9, 137.2, 136.9, 128.3, 128.12, 128.10, 128.0, 127.9, 127.8, 126.6, 126.5, 126.1, 116.93, 116.86, 115.9, 113.3, 113.0, 109.8, 59.3, 59.0, 58.7, 58.6, 57.8, 57.7, 56.6, 34.55, 34.49, 34.4, 34.4, 31.4, 31.3, 31.2, 31.1; IR (KBr) 3404 (ν_{N-H}) cm^{-1}. Anal. Calcd for $C_{112}H_{135}N_7O_7$: C, 79.54; H, 8.05; N, 5.80. Found: C, 79.24; H, 8.05; N, 5.71.

5,11,17,23,29,35,41-Hepta-*tert*-butyl-43,44,45,46,47,48,49-heptamethoxy-2,8,14,20,26,32,38-heptaazacalix[7]arene (1). A solution of **11** (198 mg, 117 μmol) and 10% $Pd(OH)_2$/C (220 mg) in cyclohexane (25 mL) was stirred at room temperature for 2 days under H_2 (3.9 atm). The reaction mixture was passed through Celite and evaporated. Flash column chromatography on silica gel (hexane/EtOAc = 4:1, v/v) furnished **1** (130 mg, 89%) as pale pink solid, mp 184−186 °C; ^{1}H NMR (500 MHz, $CDCl_3$) δ 6.90 (s, 14H, Ar−H), 6.40 (s, 7H, NH), 3.44 (s, 21H, OMe), 1.22 (s, 63H, *t*-Bu); ^{13}C NMR (125 MHz, $CDCl_3$) δ 147.0, 139.0, 138.0, 110.3, 60.0, 34.6, 31.4; IR (KBr) 3379 (ν_{N-H}) cm^{-1}; MS (FD) m/z 1240 [M$^+$]; HRMS (FD) m/z calcd for $C_{77}H_{105}N_7O_7$ 1239.8075 [M$^+$], found 1239.8047. Anal. Calcd for $C_{77}H_{105}N_7O_7\cdot$hexane: C, 75.13; H, 9.09; N, 7.39. Found: C, 74.95; H, 9.04; N, 7.09.

Gas Adsorption Experiments. By reference to the literature of Atwood and Barbour,[5c] essentially the same devise was constructed to record solid−gas absorption isotherms of **1P** at room temperature and 195 K. The powder material **1P** (25.45 mg) was placed in a sample chamber, and then both sample and reference chambers (each volume = 2.0 cm^3) were evacuated at 1 kPa for 1 h. After the chambers were pressurized to ca. 100 kPa by the desired gas, their internal pressures were monitored by using two pressure transducers attached to each chamber. Adsorption equilibrium was reached within 30 min, and the gas adsorption capacity was estimated from the changes in pressure.

Synchrotron Powder Diffraction Experiment. Powder diffraction experiments were carried out at 93 ± 1 K on a large Debye−Scherrer camera with synchrotron X-ray radiation (12.4 keV, λ = 0.99889 Å) at the BL02B2 beamline of the Super Photon Ring (SPring-8, Hyogo, Japan).[20] All calculations were performed by using a software module Reflex Plus implemented in MS Modeling version 3.2.[24] The XRD pattern of **1P** was indexed by a software X-cell[25] using 35 reflections ($3.2° < 2\theta < 12.9°$). The resultant lattice parameters were refined over the range of $2.5° < 2\theta < 40°$ by the Pawley method[26] (R_p = 0.012, R_{wp} = 0.019); the observed and simulated XRD patterns are shown in Figure S13. The space group and cell parameters of **1P** are summarized in Table 1.

X-ray Crystallographic Analysis. Measurement was made by using graphite-monochromated Mo Kα radiation (λ = 0.71075 Å). All the crystallographic calculations were performed by using a crystallographic software package, CrystalStructure version 3.8.2.[27] The crystal structure was solved by direct methods and refined by full-matrix least-squares. All non-hydrogen atoms were refined anisotropically, and hydrogen atoms were refined using the riding model except for the bridging NH hydrogen atoms whose positions were determined by D-Fourier synthesis. Crystal data for **1**·2hexane: M_r = 1413.07, monoclinic, space group $P2_1/c$ (No. 14), a = 18.458(1), b = 24.536(2), c = 19.523(1) Å, β = 101.494(2)°, V = 8664(1) Å^3, Z = 4, ρ_{calc} = 1.083 g cm^{-3}, μ = 0.679 cm^{-1}, T = 113(1) K, 18904 independent reflections, 975 refined parameters, $R1$ = 0.1167 ($I > 2\sigma(I)$), $wR2$ = 0.3759, S = 0.935. CCDC-692763 contains the supplementary crystallographic data for this paper. The data can be obtained free of charge from The Cambridge Crystallographic Data Centre via www.ccdc.cam.ac.uk/data_request/cif.

Acknowledgment. This work was supported by a Grant-in-Aid for Scientific Research (No. 19550037 to H.T.) from the Ministry of Education, Culture, Sports, Science and Technology, Japan. The synchrotron radiation experiment was performed at the BL02B2 beamline of the SPring-8 with the

(24) *MS Modeling, version 3.2*; Accelrys Inc.: San Diego, CA, 2004.
(25) Neumann, M. A. *J. Appl. Crystallogr.* **2003**, *36*, 356.
(26) Pawley, G. S. *J. Appl. Crystallogr.* **1981**, *14*, 357.
(27) *CrystalStructure, version 3.8.2*; Rigaku and Rigaku Americas: The Woodlands, TX, 2000−2007.

approval of the Japan Synchrotron Radiation Research Institute (JASRI) (Proposal No. 2008A1157). We are grateful to the GC-MS and NMR Laboratory, Faculty of Agriculture, Hokkaido University for FD MS measurements.

Supporting Information Available: ^{1}H and ^{13}C NMR spectra for all new compounds, synchrotron X-ray diffraction pattern of desolvated crystalline powder of azacalix[7]arene **1**, and a CIF file containing crystallographic data for the hexane clathrate of **1**. This material is available free of charge via the Internet at http://pubs.acs.org.

JO801543Z